J Mater Sci (2009) 44:1024–1028
DOI 10.1007/s10853-008-3225-6

Synthesis and magnetic performance of polyaniline/Mn–Zn ferrite nanocomposites with intrinsic conductivity

Jing Jiang · Lunhong Ai · Liang-Chao Li

Received: 17 October 2008 / Accepted: 22 December 2008 / Published online: 13 January 2009

Abstracts A reverse microemulsion route was employed to synthesize the electromagnetic functionalized polyaniline/$Mn_{0.6}Zn_{0.4}Fe_2O_4$ nanocomposites (PANI/MZFO NCs) using SDS/water/cyclohexane/*n*-pentanol microemulsion. The structure and morphology of obtained products were investigated by X-ray diffraction (XRD), Fourier transform infrared (FTIR) spectra, and transmission electron microscopy (TEM). The resulting nanocomposites exhibited a superparamagnetic behavior. The conductivity of MZFO nanoparticles was improved after coating with PANI. The probable formation mechanism of PANI/MZFO NCs was proposed. The prepared nanocomposites may have potential applications in magnetoelectric device.

Introduction

Organic–inorganic nanocomposites with an organized structure provide a new functional hybrid between organic and inorganic materials. Novel properties of these nanocomposites can be derived from the successful combination of the characteristics of individual constituent into a single material [1–3]. One of the most promising nanocomposites system would be the hybrids based on organic polymers and functional inorganic materials in industrial and academic fields [4–6].

Among the conducting polymers, polyaniline (PANI) has received a great deal of attention in last two decades due to its unique electrochemical and physicochemical behavior, environmental stability, and relatively easy synthesis. The attractive electrochemical and physicochemical properties result in polyaniline having various practical applications, such as corrosion protection coatings, electrocatalysts, chemical sensors, rechargeable batteries, light-emitting diodes (LEDs), and electromagnetic interference (EMI) shielding [7–12].

Recently, many interesting research has focused on the electromagnetic functionalized PANI-based nanocomposites to obtain the materials with synergetic or complementary behavior between conducting polyaniline and magnetic inorganic nanoparticles. Deng et al. have studied the synthesis of magnetic and conducting Fe_3O_4-crosslinked polyaniline nanoparticles with core-shell structure by using a precipitation–oxidation technique [13]. Yavuz et al. have reported an approach to synthesize the polyaniline–ferrite particles with a hybrid structure via an oxidative electrochemical polymerization of aniline in an aqueous solution [14]. Jacobo et al. have reported the preparation of a processible magnetite/polyaniline nanocomposite, containing dodecylbenzenesulfonic acid as a surfactant and dopant, with both magnetic and conducting properties [15]. More recently, Xu et al. have reported an in situ polymerization process to obtain polyaniline/$BaFe_{12}O_{19}$ nanocomposites and their microwave absorption properties were investigated [16]. However, up to now, the fabrication of polyaniline/ferrite nanocomposites with superparamagnetic behavior has not been reported.

Recently, reverse microemulsion polymerization has been proven to be a useful strategy for the fabrication

J. Jiang (✉) · L. Ai
Laboratory of Applied Chemistry and Pollution Control Technology, College of Chemistry and Chemical Engineering, China West Normal University, Nanchong 637002, China
e-mail: 0826zjjh@163.com

L.-C. Li
Department of Chemistry, Zhejiang Key Laboratory for Reactive Chemistry on Solid Surface, Zhejiang Normal University, Jinhua 321004, China

of polymer–inorganic nanocomposites [17]. In this work, polyaniline/$Mn_{0.6}Zn_{0.4}Fe_2O_4$ nanocomposites (PANI/MZFO NCs) with superparamagnetic behavior were synthesized by in situ polymerization of aniline in the presence of $Mn_{0.6}Zn_{0.4}Fe_2O_4$ nanoparticles (MZFO NPs) in a SDS/water/cyclohexane/*n*-pentanol quaternary microemulsion. The microstructure, morphology, and electromagnetic properties of PANI/MZFO NCs were investigated by means of various experimental techniques.

Experimental

Materials

Aniline was distilled twice under reduced pressure and stored below 0 °C. $FeCl_3$, $MnCl_2$, $ZnSO_4$, ammonium peroxydisulfate (APS, $(NH_4)_2S_2O_8$), cyclohexane, *n*-pentanol, sodium dodecyl sulfate (SDS) were all of analytical purity and used without further purification.

Preparation of MZFO NPs colloidal suspension

An aqueous MZFO NPs colloidal suspension was prepared according to the ferrofluid process developed by Massart [18]. In a typical procedure, stoichiometric amounts of $FeCl_3$, $MnCl_2$, and $ZnSO_4$ were dissolved in 50 mL distilled water. Then, the obtained mixture solution was poured as quickly as possible into the boiling solution of NaOH (200 mL, 0.625 mol L^{-1}). The boiling temperature was maintained during 2 h. The precipitate was separated from the supernatant by magnetic decantation and washed three times with distilled water. To create sufficient electrostatic repulsion between particles, the precipitate particles were then dispersed in nitric acid (100 mL, 2 mol L^{-1}) during 15 min under vigorous stirring. Then the acidic precipitate was isolated by decantation on a magnet, washed with acetone for three times. The resulting precipitate particles were finally dispersed in water (50 mL) and the residue of acetone was eliminated under vacuum at 60 °C. A stable MZFO NPs colloidal suspension was obtained.

Preparation of PANI/MZFO NCs

The syntheses of PANI/MZFO NCs were simply achieved via a microemulsion route. A quaternary microemulsion, SDS/water/cyclohexane/*n*-pentanol, was selected for this study. Cyclohexane was used as the oil phase, SDS as surfactant, *n*-pentanol as co-surfactant, and an aqueous solution as the dispersed phase. In a typical procedure, 1.5 g SDS was added into 5 mL 0.1 mol L^{-1} HCl solution, then 1 mL *n*-pentanol and 50 mL cyclohexane were introduced. The mixture was stirred and the system became transparent immediately; thus, a clear and transparent microemulsion system was obtained. A certain amount of MZFO NPs colloidal suspension was added into the homogeneous solution and sonicated for 1 h. Then, 1 mL aniline monomer was added to the suspension and stirred for 30 min, and 5 mL deionized water containing 2.49 g ammonium persulfate was then slowly added dropwise to the well-stirred reaction mixture. After a few minutes, the suspension became green, indicating polymerization of aniline. The reaction was carried out at 0 °C under nitrogen while stirring for 8 h. The nanocomposites were obtained by filtering and washing the suspension with methanol and water, and dried under vacuum at 60 °C for 24 h.

Characterization

X-ray diffraction (XRD) patterns of the samples were collected on a Philips X'pert Pro MPD X-ray diffractometer with Cu Kα radiation ($\lambda = 0.15418$ nm). FT-IR spectra were recorded on a Nicolet Avatar 360 spectrometer in the range of 400–2000 cm^{-1} using KBr pellets. TEM images were carried out on a JEOL JEM-2010 transmission electron microscope at an accelerating voltage of 200 kV. The room temperature direct current (dc) conductivity was measured by standard four-probe methods using a programmable SDY-5 DC voltage/current detector (Guangzhou Semiconductor Institute, China). All dry powder samples were pressed into disk pellets with 15 mm in diameter and 0.8 mm in thickness. Magnetic measurements were carried out at room temperature using a vibrating sample magnetometer (VSM, Lakeshore 7404) with a maximum magnetic field of 5 kOe. The temperature-dependant magnetization was measured by Superconducting Quantum Interference Device (SQUID).

Results and discussions

Structural characterization and morphology of PANI/MZFO NCs

The phase identification of the as-prepared sample has been determined by XRD. Figure 1 shows the XRD patterns of MZFO NPs, PANI/MZFO NCs, and pristine PANI. It is observed from Fig. 1a that the XRD pattern of MZFO NPs presents the single-phase spinel structure with no extra reflections, and the diffraction peaks can be well indexed to (111), (220), (311), (222), (400), (422), (511), and (440) crystal plane of cubic spinel. As shown in Fig. 1b, it is clearly seen that both the characteristic peaks of PANI centred at around $2\theta = 20.4°$, 25.1°, and MZFO NPs appear in the XRD patterns of the nanocomposite. Also, the

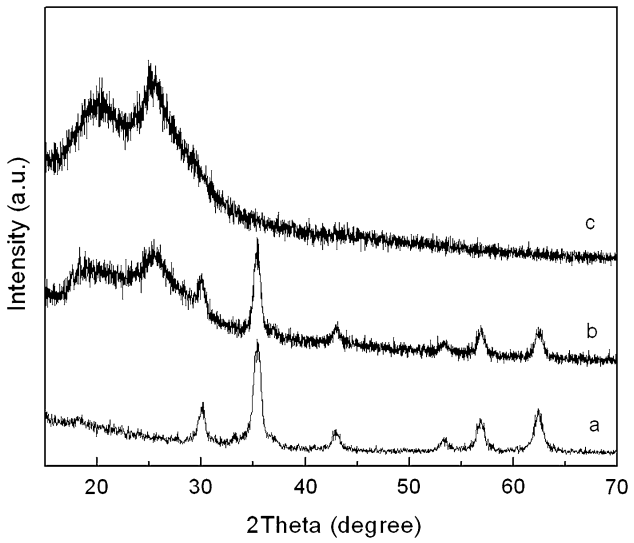

Fig. 1 XRD patterns of MZFO NPs (a), PANI/MZFO NCs (b), and PANI (c)

intensities of the characteristic peaks of PANI become more weaker after introducing MZFO NPs into the polymer matrix, revealing the crystallinity of PANI in the nanocomposites is much lower than that of the pristine PANI.

The FTIR spectra measurement was carried out to study the molecular structure of the nanocomposites. Figure 2 shows the FTIR spectra of the pristine PANI and PANI/MZFO NCs. For the pristine PANI (Fig. 2a), the characteristic peaks appear at 1569 cm^{-1} (C=C stretching of the quinoid rings), 1483 cm^{-1} (C=C stretching of the benzenoid rings), 1303 and 1249 cm^{-1} (C–N stretching modes of the benzenoid ring), 1139 cm^{-1} (C–H in-plane bending modes), and 800 cm^{-1} (C–H out-of-plane bending modes). The FTIR spectrum of PANI/MZFO NCs (Fig. 2b) is almost identical to that of the pristine PANI. In addition,

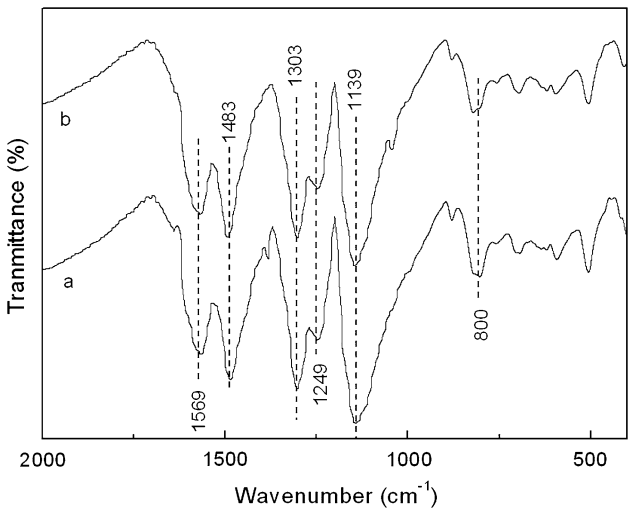

Fig. 2 FTIR spectra of PANI (a) and PANI/MZFO NCs (b)

there are no characteristic peaks of MZFO NPs in the FTIR spectra of nanocomposites, indicating the well wrapping of MZFO NPs with PANI in the nanocomposites [19].

The morphology and particle sizes were determined by means of TEM. Figure 3 shows the TEM images of MZFO NPs and PANI/MZFO NCs. For the MZFO NPs, the very fine particles with the size range from 13 to 18 nm are observed from Fig. 3a; moreover, a certain degree of agglomeration also appears due to interaction between magnetic nanoparticles. It can be clearly seen from Fig. 3b that black-colored MZFO NPs are well-dispersed in the light-colored PANI matrix, and the degree of agglomeration is reduced significantly.

Electrical and magnetic properties of PANI/MZFO NCs

The room temperature dc conductivity of PANI/NZFO NCs is affected significantly by the introduction of NZFO NPs into polymer matrix. The dc conductivity of the pristine PANI is 0.54 S/cm, while that of PANI/NZFO NCs is reduced to 0.08 S/cm. A great decrease in conductivity can be considered as follows: (1) the insulting behavior of MZFO NPs in the nanocomposites; (2) from XRD study, the introduction of MZFO NPs would weaken the crystallinity of PANI.

Figure 4 shows the hysteresis loops of MZFO NPs and PANI/MZFO NCs. For MZFO NPs, the absence of hysteresis, immeasurable remanence, and coercivity indicate the presence of superparamagnetic behavior, which is attributed to the size of equiaxial-shaped nanoparticles below the superparamagnetic critical size. It is found that the magnetization of PANI/MZFO NCs also exhibits a clear superparamagnetic behavior, suggesting that the size of MZFO NPs in PANI matrix is smaller than the superparamagnetic critical size. The magnetic domain size for PANI/MZFO NCs can be calculated from the magnetization curves using the following formula [20, 21]:

$$D_{\mathrm{m}} = \frac{18k_{\mathrm{B}}T}{\pi}\frac{\chi_i}{M_{\mathrm{S}}^2} \quad (1)$$

where χ_i is the initial magnetic susceptibility (slope M/H), k_{B} is the Boltzmann constant, T is the absolute temperature, and M_{S} is saturation magnetization. The obtained magnetic domain size (D_{m}) at 300 K is smaller than the morphological size (determined by TEM measurement) due to the formation of a disordered nonmagnetic surface layer, which is similar to the results reported in the previous literatures [22–24].

According to Stoner–Wohlfarth theory, magnetic anisotropy (E_{A}) energy for single-domain particles can be expressed as

$$E_{\mathrm{A}} = KV\sin^2\theta \quad (2)$$

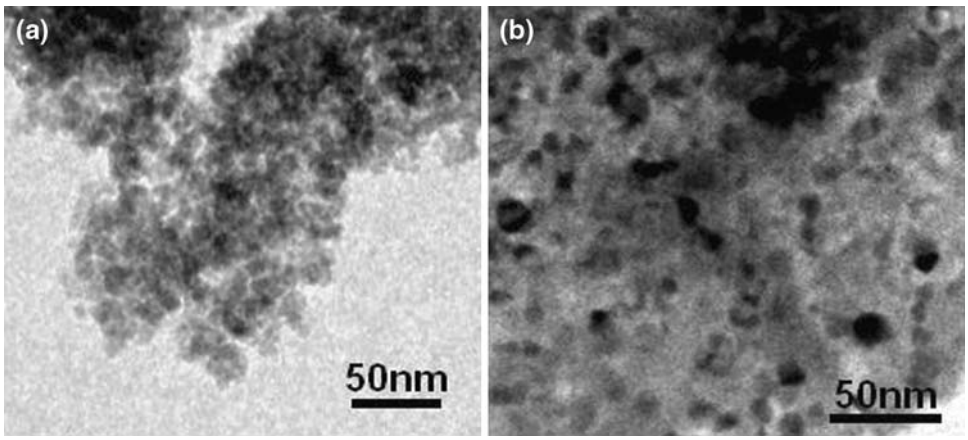

Fig. 3 TEM images of MZFO NPs (**a**) and PANI/MZFO NCs (**b**)

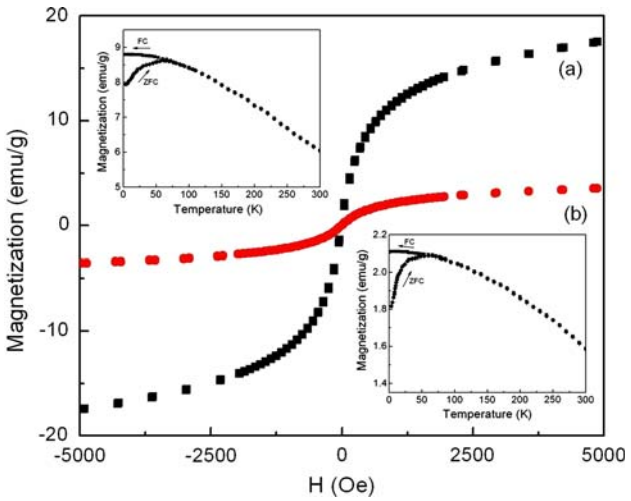

Fig. 4 Hysteretic loops of MZFO NPs (a) and PANI/MZFO NCs (b); temperature-dependent magnetization (ZFC/FC) of MZFO NPs (*upper-left inset*) and PANI/MZFO NCs (*lower-right inset*) measured at a magnetic field of 500 Oe

where K is the magnetic anisotropy constant, V is the volume of the nanoparticle, and θ is the angle between magnetization direction and the easy axis of the nanoparticle [25]. The anisotropy represents the energy barrier to prevent the change of the magnetization direction. When the nanoparticles size is reduced to a threshold value, E_A is less than the thermal activation energy. Consequently, the magnetization direction of nanoparticle is easily moved away from the easy axis due to thermal activation, resulting in the superparamagnetic phenomenon. In addition, the observed decrease in M_S of MZFO NPs upon coating with PANI can be attributed to the nonmagnetic PANI contribution to the total magnetization. Insets in Fig. 4 display the temperature dependence magnetization curves measured at a magnetic field of 500 Oe. For MZFO NPs and PANI/MZFO NCs, the ZFC magnetization at low temperature is much lower than the FC magnetization. Under ZFC conditions, the particles become magnetically frozen, and their magnetic moment could not flip and align rapidly along the direction of the applied field. The spins become able to flip only above the blocking temperature (T_B) [26] and the ZFC magnetization then coincides with the FC magnetization. The blocking temperature T_B is around 64 K for MZFO NPs and 52 K for PANI/MZFO NCs in an applied field of 500 Oe. A decrease in the blocking temperature after coating with PANI can be considered that the polymer matrix allows each ferrite nanoparticle to behave independently and interparticle interactions are not important [27], which is similar to the results reported in the literature [15, 19, 28].

Formation mechanism

On the basis of basic concepts of polymerization and well supported by TEM measurements of the as-prepared PANI/MZFO NCs, the probable formation mechanism was proposed and depicted schematically in Fig. 5. In this study, SDS (surfactant), *n*-pentanol (co-surfactant) are employed to solubilize aqueous microdroplets in the microemulsion system. Each microdroplet, in which ferrite nanoparticles are homogeneously suspended, provides an ideal environment for reaction, acting as nanoreactor. It is known that the surface charge of metal oxide is positive below the pH of the point of zero charge (PZC), while it is negative above that. Since the surface of magnetite has PZC of pH $\approx$ 6 [29], it is positively charged in the acidic conditions. Therefore, adsorption of an amount of the anions such as Cl^- may occur and compensate the positive charges on ferrite surface. In addition, the specific adsorption of these anions on the ferrite surface may also take place. In this approach, aniline monomers are converted to cationic anilinium ions in acidic conditions. Thus, the electrostatic interactions appear between anions adsorbed on the ferrite surface and cationic anilinium ions. The aniline monomers electrostatically complexed to the ferrite surface are then polymerized by ammonium persulfate as an oxidizing

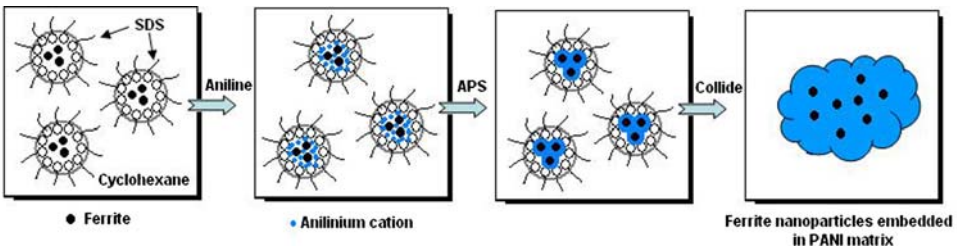

Fig. 5 Proposed mechanism for the formation of PANI/MZFO NCs

agent. The products are obtained by washing with methanol and water to remove surfactants and initiators.

Conclusions

In summary, the electrical magnetic multifunctional PANI/MZFO NCs were successfully synthesized by in situ polymerization of aniline in the presence of MZFO NPs in SDS/water/cyclohexane/*n*-pentanol quaternary microemulsion. It was shown that the MZFO NPs were embedded in PANI matrix. The room temperature conductivity of NZFO NPs was improved after PANI coating. PANI/MZFO NCs under applied magnetic field exhibited superparamagnetic behavior. The observed decrease in M_S for PANI/MZFO NCs is due to the nonmagnetic PANI contribution to the total magnetization. The prepared nanocomposites may have potential applications in magnetoelectric devices.

Acknowledgement This work was supported by Scientific Research Foundation of China West Normal University (07B008, 07B005).

References

1. Zhang XZ, Huang YD, Wang TY et al (2007) J Mater Sci 42:5264. doi:10.1007/s10853-006-0349-4
2. Zhao LJ, Yang H, Cui Y et al (2007) J Mater Sci 42:4110. doi:10.1007/s10853-006-0876-z
3. Qian JH, Guo CY, Wang H et al (2007) J Mater Sci 42:4350. doi:10.1007/s10853-006-0692-5
4. Utracki LA, Sepehr M, Boccaleri E (2007) Polym Adv Technol 18:1
5. Liu ZL, Liu PD, Liu CC et al (2007) J Mater Sci 42:5147. doi:10.1007/s10853-006-1284-0
6. Mack JJ, Cox BN, Lee M et al (2007) J Mater Sci 42:6139. doi:10.1007/s10853-006-0982-y
7. Ahmad N, MacDiarmid AG (1996) Synth Met 78:103
8. Ficicoglu F, Kadirgan F (1998) J Electroanal Chem 451:95
9. Kan JQ, Pan XH, Chen C (2004) Biosens Bioelectron 19:1635
10. Kuwabata S, Masui S, Yoneyama H (1999) Electrochim Acta 44:4593
11. Wang HL, MacDiarmid AG, Wang Y et al (1996) Synth Met 78:33
12. Mäkelä T, Pienimaa S, Taka T (1997) Synth Met 85:1335
13. Deng J, Ding X, Zhang W et al (2002) Polymer 43:2179
14. Yavuz Ö, Ram MK, Aldissi M et al (2005) J Mater Chem 15:810
15. Aphesteguy JC, Jacobo SE (2007) J Mater Sci 42:7062. doi:10.1007/s10853-006-1423-7
16. Xu P, Han X, Jiang J et al (2007) J Phys Chem C 111:12603
17. Sui X, Chu Y, Xing S et al (2004) Mater Lett 58:1255
18. Zins D, Cabuil V, Massart R (1999) J Mol Liq 83:217
19. Li G, Yan S, Zhou E et al (2006) Colloids Surf A 276:40
20. Massart R (1981) IEEE Trans Magn 17:1247
21. Sertkol M, Köseoğlu Y, Baykal A et al (2009) J Magn Magn Mater 321:157
22. Leslie-Pelecky DL, Rieke RD (1996) Chem Mater 8:1770
23. Blanco-Mantecon M, O'Grady K (2006) J Magn Magn Mater 296:124
24. Turcu R, Pana O, Nan A et al (2008) J Phys D Appl Phys 41:245002
25. Stoner EC, Wohlfarth EP (1991) IEEE Trans Magn 27:3475
26. Neel L (1953) Rev Mod Phys 25:293
27. Lyon JL, Fleming DA, Stone MB et al (2004) Nano Lett 4:719
28. Grasset F, Labhsetwar N, Li D et al (2002) Langmuir 18:8209
29. Sun ZX, Su FW, Forsling W et al (1998) J Colloid Interface Sci 197:151